Lawrence Berkeley National Laboratory
Recent Work

Title
Unique Energy Alignments of a Ternary Material System toward High-Performance Organic Photovoltaics.

Permalink

Journal

ISSN

Authors
Cheng, Pei
Wang, Jiayu
Zhang, Qianqian
et al.

Publication Date

DOI

Peer reviewed

COMMUNICATION

Organic Solar Cells

ADVANCED
MATERIALS

www.advmat.d

Check for
updates

Unique Energy Alignments of a Ternary Material System toward High-Performance Organic Photovoltaics

Pei Cheng, Jiayu Wang, Qianqian Zhang, Wenchao Huang, Jingshuai Zhu, Rui Wang, Sheng-Yung Chang, Pengyu Sun, Lei Meng, Hongxiang Zhao, Hao-Wen Cheng, Tianyi Huang, Yuqiang Liu, Chaochen Wang, Chenhui Zhu, Wei You,* Xiaowei Zhan,* and Yang Yang*

Incorporating narrow-bandgap near-infrared absorbers as the third component in a donor/acceptor binary blend is a new strategy to improve the power conversion efficiency (PCE) of organic photovoltaics (OPV). However, there are two main restrictions: potential charge recombination in the narrow-gap material and miscompatibility between each component. The optimized design is to employ a third component (structurally similar to the donor or acceptor) with a lowest unoccupied molecular orbital (LUMO) energy level similar to the acceptor and a highest occupied molecular orbital (HOMO) energy level similar to the donor. In this design, enhanced absorption of the active layer and enhanced charge transfer can be realized without breaking the optimized morphology of the active layer. Herein, in order to realize this design, two new narrow-bandgap nonfullerene acceptors with suitable energy levels and chemical structures are designed, synthesized, and employed as the third component in the donor/acceptor binary blend, which boosts the PCE of OPV to 11.6%.

Photovoltaic (PV) technology is one of the promising renewable energy technologies for the human future. Especially, the solution-processable organic photovoltaics (OPV) have attracted considerable attention in the last decade due to some potential advantages, such as light-weight, flexibility, possible semitransparence, low energy consumption, and fast and large-area fabrication.[1–6] To date, OPV have shown the best performance with certified power conversion efficiency (PCE) exceeding 11%.[7]

Research on OPV has begun in as early as 1950s, when the active layer consisted of only a single organic semiconductor (p-type or n-type).[8] Considering the large binding energy of an organic semiconductor (≈0.3–1 eV),[9] the single component OPV yielded a very low PCE (≈1–3%) due to the insufficient exciton dissociation by the electric field. To overcome this problem, the active layer consisted of donor/acceptor binary blend (bulk heterojunction (BHJ) structure) was reported in 1995.[10,11] In this binary blend OPV, the exciton dissociation became much more efficient than that in the single component solar cells due to the increased donor/acceptor interfaces in the active layer. In recent five years, a new type of active layer with ternary blend (donor, acceptor, and third component) was developed to further enhance the performance of binary blend OPV.[12–15] These ternary blend OPV presented some advantages via various design strategies: broader and stronger absorption,[16–25] more efficient charge transfer,[26–29] more efficient charge transport pathways,[30–33] better charge extraction at the electrodes,[34–37] and improved stability.[38–42]

Among the design strategies for ternary blend OPV, employing a near-infrared (NIR) absorber as the third component is the most successful one to boost the PCE of

Dr. P. Cheng, Dr. W. Huang, R. Wang, S.-Y. Chang, P. Sun, Dr. L. Meng, H. Zhao, H.-W. Cheng, T. Huang, Y. Liu, C. Wang, Prof. Y. Yang
Department of Materials Science and Engineering
University of California
Los Angeles, CA 90095, USA
E-mail: yangy@ucla.edu

J. Wang, J. Zhu, Prof. X. Zhan
Department of Materials Science and Engineering
College of Engineering
Key Laboratory of Polymer Chemistry and Physics of Ministry of Education
Peking University
Beijing 100871, P. R. China
E-mail: xwzhan@pku.edu.cn

Q. Zhang, Prof. W. You
Department of Chemistry
University of North Carolina at Chapel Hill
Chapel Hill, NC 27599, USA
E-mail: wyou@unc.edu

Dr. W. Huang, H. Zhao, H.-W. Cheng, Y. Liu, Prof. Y. Yang
California NanoSystems Institute
University of California
Los Angeles, CA 90095, USA

Dr. C. Zhu
Advanced Light Source
Lawrence Berkeley National Laboratory
Berkeley, CA 94720, USA

ADVANCED
SCIENCE NEWS
www.advancedsciencenews.com

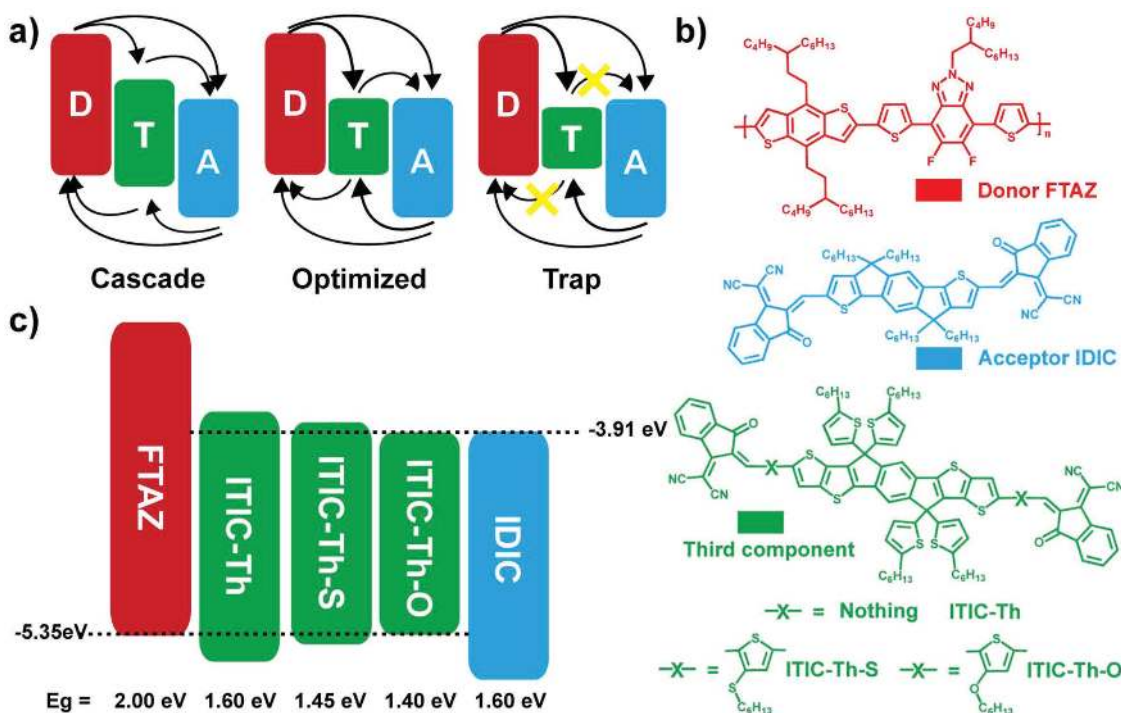ADVANCED
MATERIALS
www.advmat.de

Figure 1. a) Schematic diagrams of different models for charge transfer. b) Molecular structures of donor (FTAZ), acceptor (IDIC), and third components (ITIC-Th, ITIC-Th-S, ITIC-Th-O). c) Energy levels and optical bandgaps of FTAZ, IDIC, ITIC-Th, ITIC-Th-S, and ITIC-Th-O.

OPV. These NIR absorbers, including donors[16–22,26] and acceptors,[23,43–46] can utilize photons in the NIR region, which will potentially contribute to the short circuit current density (J_{SC}) of solar cells. On the other hand, the highest occupied molecular orbital (HOMO) and lowest unoccupied molecular orbital (LUMO) energy levels of NIR absorbers can be designed to be positioned between the HOMOs and LUMOs of the donor and acceptor, which can provide more routes for charge transfer by forming a cascade energy heterojunction (**Figure 1**a).[47] However, there are two main restrictions for the application
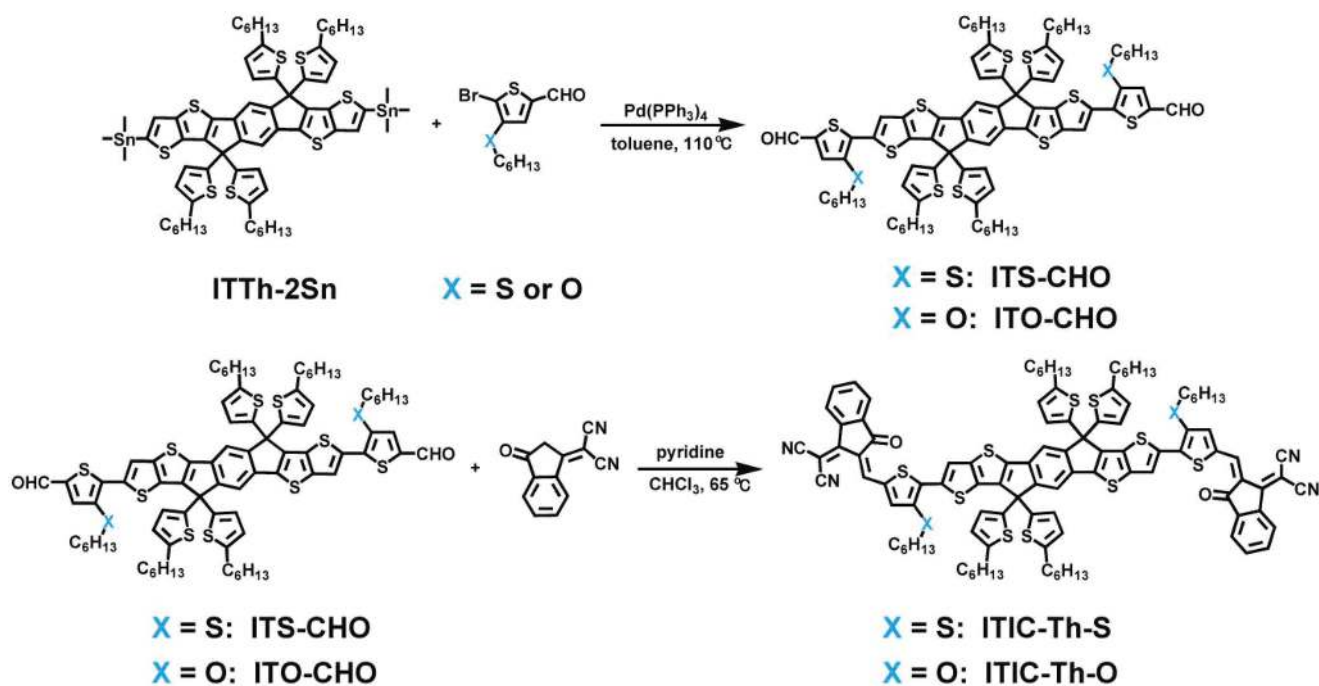

Figure 2. The synthetic routes of ITIC-Th-S and ITIC-Th-O.

**ADVANCED
SCIENCE NEWS**

www.advancedsciencenews.com
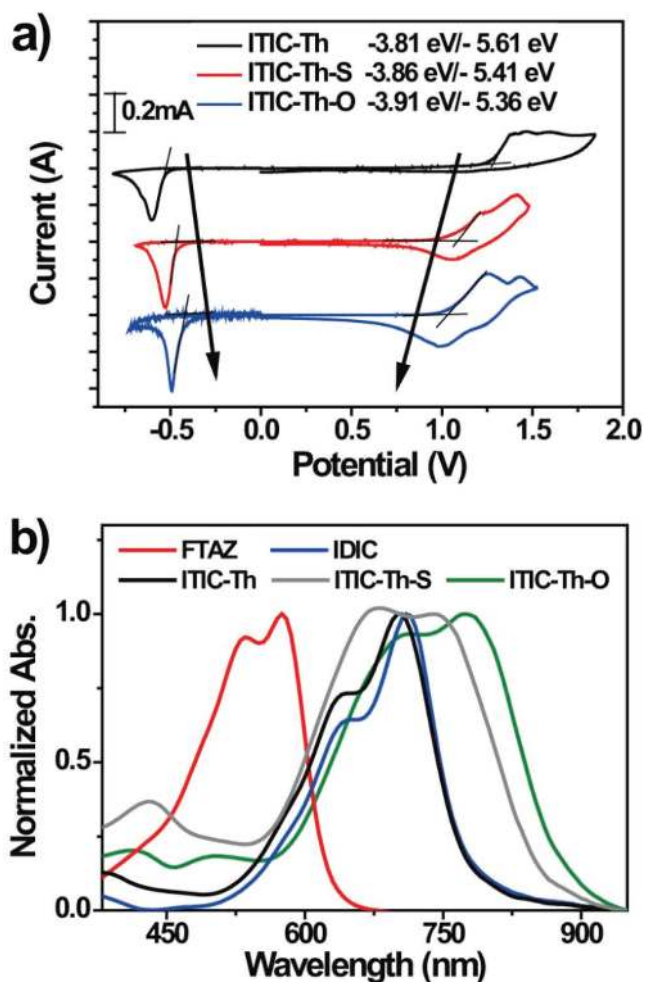
**ADVANCED
MATERIALS**

www.advmat.de

Figure 3. a) Cyclic voltammograms for ITIC-Th, ITIC-Th-S, and ITIC-Th-O. b) Absorption spectra of pure FTAZ, IDIC, ITIC-Th, ITIC-Th-S, and ITIC-Th-O films.

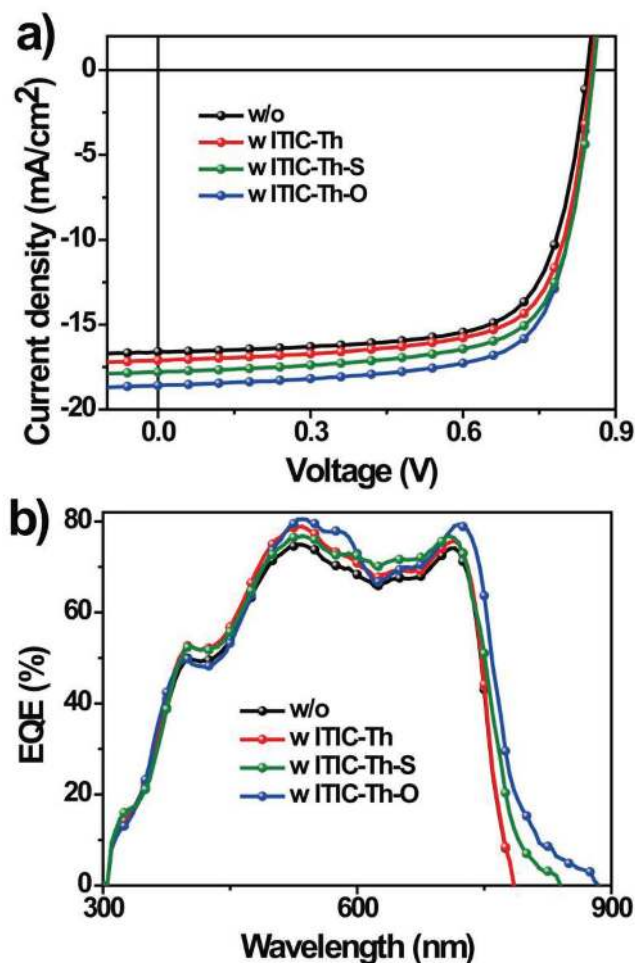**Figure 4.** a) J–V curves and b) EQE spectra of devices based on FTAZ/IDIC without or with different third components under illumination of an AM 1.5G solar simulator, 100 mW cm⁻².

of NIR absorbers as the third component: potential charge recombination in the narrow gap material and miscompatibility between each component.[12,14,15] The charge recombination traps can be formed if the bandgap of the third component is too narrow (Figure 1a). The miscompatibility occurs if the chemical structures of donor/acceptor and the third component are mainly different, which will break the optimized morphology of the donor/acceptor binary blend active layer.[48] Thus, the optimized design is to employ a third component (structurally similar to donor or acceptor) with a LUMO energy level similar to the acceptor and a HOMO energy level similar to the donor (Figure 1a). In this design, enhanced absorption of active layer and enhanced charge transfer can be realized without the breaking of the optimized morphology of active layer.

Herein, in order to realize this optimized design of ternary blend OPV, we employed the third component in the active layer with a similar chemical structure to the acceptor and suitable energy levels. On the basis that 2,7-bis(3-dicyanomethylene-2Z-methylene-indan-1-one)-4,4,9,9-tetrakis(5-hexylthiophen-2-yl)-4,9-dihydro-s-indaceno[1,2-b:5,6-b']di(thieno[3,2-b]thiophene) (ITIC-Th)[49,50] shows a similar backbone and

bandgap (1.60 eV), but up-shifted LUMO and HOMO energy levels to 2,7-bis(3-dicyanomethylene-2Z-methylene-indan-1-one)-4,4,9,9-tetrahexyl-4,9-dihydro-s-indaceno[1,2-b:5,6-b']-dithiophene (IDIC), ITIC-Th was chosen as the third component in the blend of donor FTAZ[51]/acceptor IDIC.[52,53] In order to achieve optimized energy level alignments of ITIC-Th-based third component with the donor FTAZ/acceptor IDIC, 2,7-bis(5-(3-dicyanomethylene-2Z-methylene-indan-1-one)-3-hexylthio-thiophene-2-yl)-4,4,9,9-tetrakis(5-hexylthiophen-2-yl)-4,9-dihydro-s-indaceno[1,2-b:5,6-b']di(thieno[3,2-b]thiophene) (ITIC-Th-S), and 2,7-bis(5-(3-dicyanomethylene-2Z-methylene-indan-1-one)-3-hexyloxy-thiophene-2-yl)-4,4,9,9-tetrakis(5-hexylthiophen-2-yl)-4,9-dihydro-s-indaceno[1,2-b:5,6-b']di(thieno[3,2-b]thiophene) (ITIC-Th-O) (Figure 1b) were designed and synthesized through the incorporation of thiophene with alkylthio/alkoxy side chains as pi-bridge. This approach could down-shift the LUMO energy level and up-shift the HOMO energy level of the ITIC-Th counterpart and, therefore, redshift the absorption into the NIR region (bandgaps: 1.45 eV for ITIC-Th-S and 1.40 eV for ITIC-Th-O, as shown in Figure 1c). Through this chemical modification, the HOMO

**ADVANCED
SCIENCE NEWS**
www.advancedsciencenews.com

**ADVANCED
MATERIALS**
www.advmat.de

Table 1. Average and best device data based on FTAZ/IDIC without or with different third components.

Active layer	V_{OC} [V]	J_{SC} [mA cm^{-2}]	Calculated J_{SC} [mA cm^{-2}]	FF [%]	PCE [%]	
					Average	Best
FTAZ/IDIC	0.85 ± 0.01	16.6 ± 0.5	15.9	71.0 ± 0.4	10.0 ± 0.3	10.4
FTAZ/ITIC-Th/IDIC	0.85 ± 0.01	17.1 ± 0.4	16.5	70.9 ± 0.5	10.3 ± 0.2	10.6
FTAZ/ITIC-Th-S/IDIC	0.85 ± 0.01	17.8 ± 0.5	17.1	71.2 ± 0.4	10.8 ± 0.2	11.1
FTAZ/ITIC-Th-O/IDIC	0.85 ± 0.01	18.5 ± 0.4	18.0	71.9 ± 0.4	11.3 ± 0.2	11.6

and the LUMO energy levels of ITIC-Th-O were respectively similar to the HOMO energy level of donor FTAZ (−5.35 eV) and the LUMO energy level of acceptor IDIC (−3.91 eV). After the device optimization, the best PCE of FTAZ/ITIC-Th-O/IDIC ternary blend OPV was measured to be 11.6%, which is higher than that of the controlled FTAZ/IDIC binary blend OPV (10.4%).

The synthetic routes of ITIC-Th-S and ITIC-Th-O are shown in **Figure 2**. The intermediate compounds 5,5′-(4,4,9,9-tetrakis(5-hexylthiophen-2-yl)-4,9-dihydro-*s*-indaceno[1,2-*b*:5,6-*b*′]di(thieno[3,2-*b*]thiophene)-2,7-diyl)bis(4-(hexylthio)thiophene-2-carbaldehyde) (ITS-CHO)/5,5′-(4,4,9,9-tetrakis(5-hexylthiophen-2-yl)-4,9-dihydro-*s*-indaceno[1,2-*b*:5,6-*b*′]di(thieno[3,2-*b*]thiophene)-2,7-diyl)bis(4-(hexyloxy)thiophene-2-carbaldehyde) (ITO-CHO) were synthesized in 83%/71% yield through the Stille coupling reaction using Pd(PPh₃)₄ as a catalyst. A straightforward reaction of ITS-CHO/ITO-CHO with 1,1-dicyanomethylene-3-indanone afforded ITIC-Th-S/ITIC-Th-O in 76%/95% yield. The compounds ITS-CHO/ITO-CHO and ITIC-Th-S/ITIC-Th-O were fully characterized by MALDI-TOF MS, ^{1}H NMR, ^{13}C NMR, and elemental analysis. ITIC-Th-S and ITIC-Th-O were readily soluble in common organic solvents such as chloroform and o-dichlorobenzene at room temperature. The details of synthesis and related characterization are shown in the Supporting Information.

The cyclic voltammetry (CV) method was used to investigate the electrochemical properties of ITIC-Th, ITIC-Th-S, and ITIC-Th-O films and further estimate their energy levels (**Figure 3**a). The HOMO/LUMO energy levels of ITIC-Th-S and ITIC-Th-O were estimated to be −5.41 eV/−3.86 eV and −5.36 eV/−3.91 eV, respectively (calculation details were shown in the Supporting Information). Due to electron-donating nature of alkylthio/alkoxy side chains and high electronegativity of sulfur (2.58) and oxygen atoms (3.44), ITIC-Th-S and ITIC-Th-O exhibited an up-shifted HOMO energy levels and down-shifted LUMO energy levels compared with ITIC-Th (−5.61 eV/−3.81 eV). Through this simple chemical modification, the LUMO energy level of the third component can be down-shifted from −3.81 to −3.91 eV, which is similar to that of the acceptor IDIC (−3.91 eV[49]); and the HOMO energy level of the third component can be up-shifted from −5.61 to −5.36 eV, which is similar to that of the donor FTAZ (−5.35 eV, Figure S1, Supporting Information). Meanwhile, the down-shifted LUMO energy level and up-shifted HOMO energy level of the third component can narrow the bandgap and broaden the absorption of active layer into the NIR region. The absorption spectra of FTAZ, IDIC, ITIC-Th, ITIC-Th-S, and ITIC-Th-O films are shown in Figure 3b. Compared with ITIC-Th, ITIC-Th-S, and

ITIC-Th-O exhibit redshifted absorptions (855 and 885 nm) and reduced bandgaps (1.45 and 1.40 eV). The redshifted absorption of the third component can potentially benefit the absorption of the ternary blend active layer, which is only cut-off at 775 nm for the FTAZ/IDIC binary blend (1.60 eV).

The J–V curves and external quantum efficiency (EQE) spectra of devices based on FTAZ/IDIC without or with different third components (ITIC-Th, ITIC-Th-S, and ITIC-Th-O) under the illumination of an AM 1.5 G solar simulator (100 mW cm^{-2}) are shown in **Figure 4**. The average (calculated from 20 individual devices) and best device characteristics are summarized in **Table 1**. The device characteristics of FTAZ/ITIC-Th, FTAZ/ITIC-Th-S, and FTAZ/ITIC-Th-O binary blend solar cells are also summarized in Table S1 (Supporting Information). After addition of third component (10% of the donor and acceptor by weight), the ternary blend OPV exhibited an enhanced J_{SC} with maintaining an open circuit voltage (V_{OC}) (≈0.85 V) and fill factor (FF) (≈0.71) comparable to controlled FTAZ/IDIC binary blend device. The average J_{SC} of devices increased from 16.6 to 17.8 and 18.5 mA cm^{-2} by employing ITIC-Th-S and ITIC-Th-O as the third component, respectively. As a result, the best PCE of the devices increased from 10.4% to 11.1% and 11.6% by incorporation of ITIC-Th-S and ITIC-Th-O as the third component, respectively. The best ternary blend OPV was based on ITIC-Th-O as a third component, which showed similar LUMO energy level to acceptor IDIC (−3.91 eV) and similar HOMO energy level to donor FTAZ (−5.35 eV). In addition, PCE (≈11%) and FF (≈70%) of ternary blend device can be mainly maintained by continuous increasing the
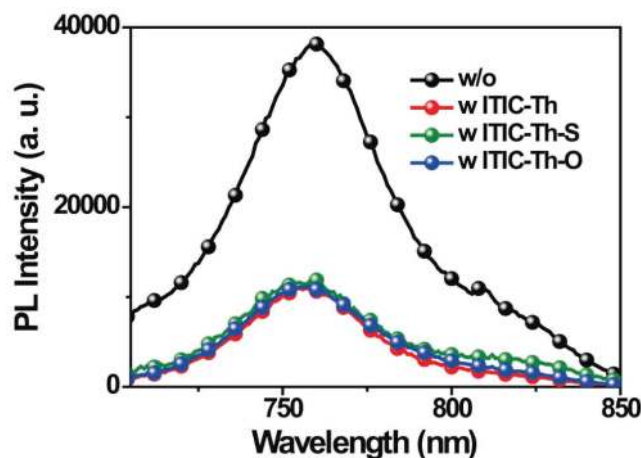

Figure 5. PL spectra of FTAZ/IDIC blend films without or with different third components.

**ADVANCED
SCIENCE NEWS**

www.advancedsciencenews.com
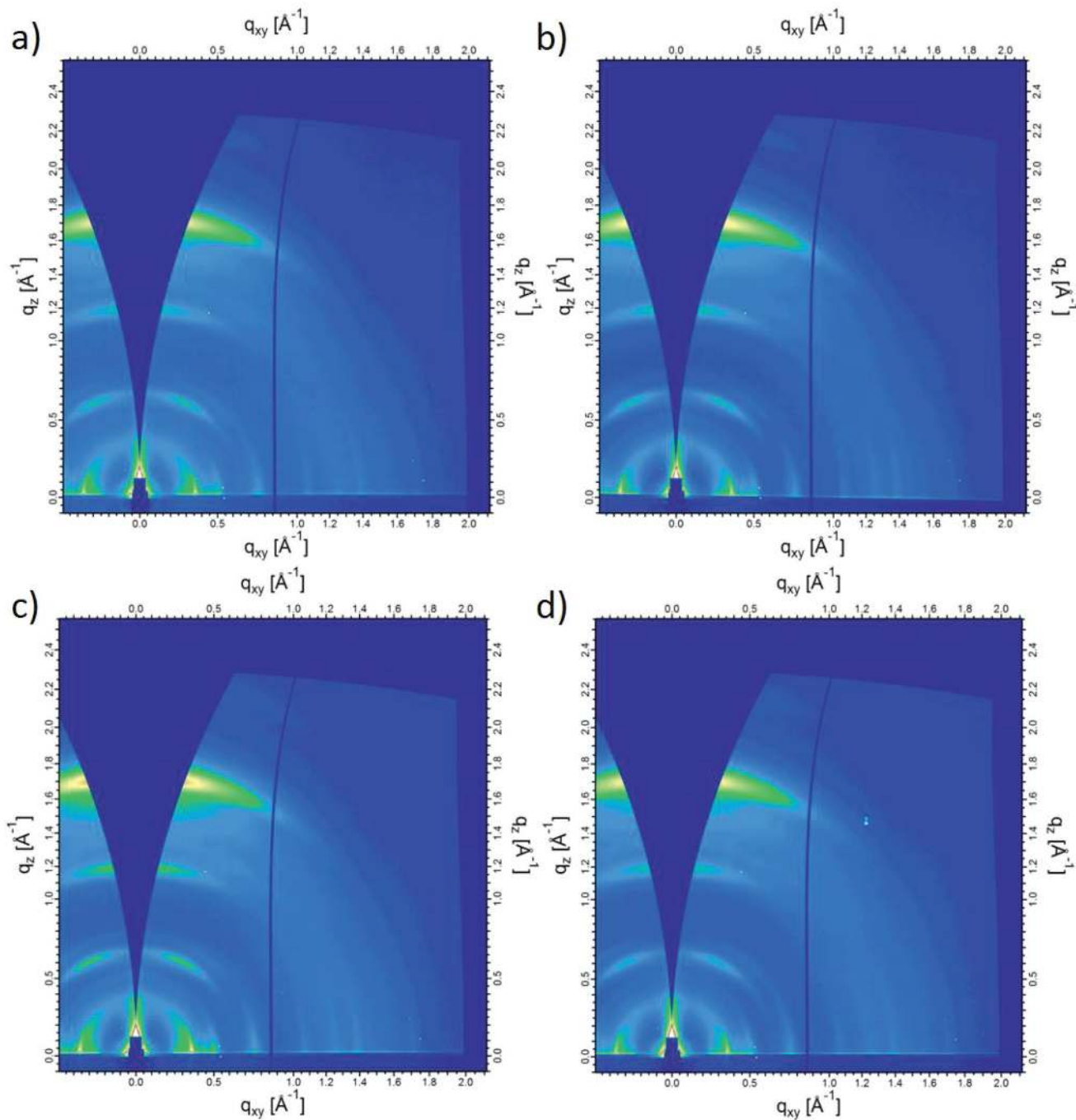
**ADVANCED
MATERIALS**

www.advmat.de

Figure 6. a–d) 2D GIWAXS patterns of FTAZ/IDIC film (a), FTAZ/ITIC-Th/IDIC film (b), FTAZ/ITIC-Th-S/IDIC film (c), and FTAZ/ITIC-Th-O/IDIC film (d).

amount of third component (up to 30%, Table S2, Supporting Information).

As shown in Figure 4b and Figure 3b, the EQE in 400–600 nm range is attributed mainly to FTAZ, and the EQE in 600–750 nm range is attributed mainly to IDIC. After the addition of ITIC-Th-S or ITIC-Th-O as the third component, the EQE can be broadened to 850 or 880 nm, which is consistent with the absorption spectra of blend films (Figure S2, Supporting information). From integration of the EQE spectra with the AM 1.5G reference spectrum, the calculated J_{SC} was

obtained, which was similar to J–V measurement (the average error is 3.6%, Table 1).

In order to study the charge or energy transfer between different components, we carry out the same method as literatures (investigating the J–V curves of solar cells based on two acceptors as active layer (without donor).[20,54] J–V curves of devices based on pure IDIC, pure ITIC-Th-O, and IDIC/ITIC-Th-O blend under illumination of an AM 1.5G solar simulator, 100 mW cm^{-2} are shown in Figure S3 (Supporting information). The J_{SC} of solar cells based on IDIC/ITIC-Th-O blend
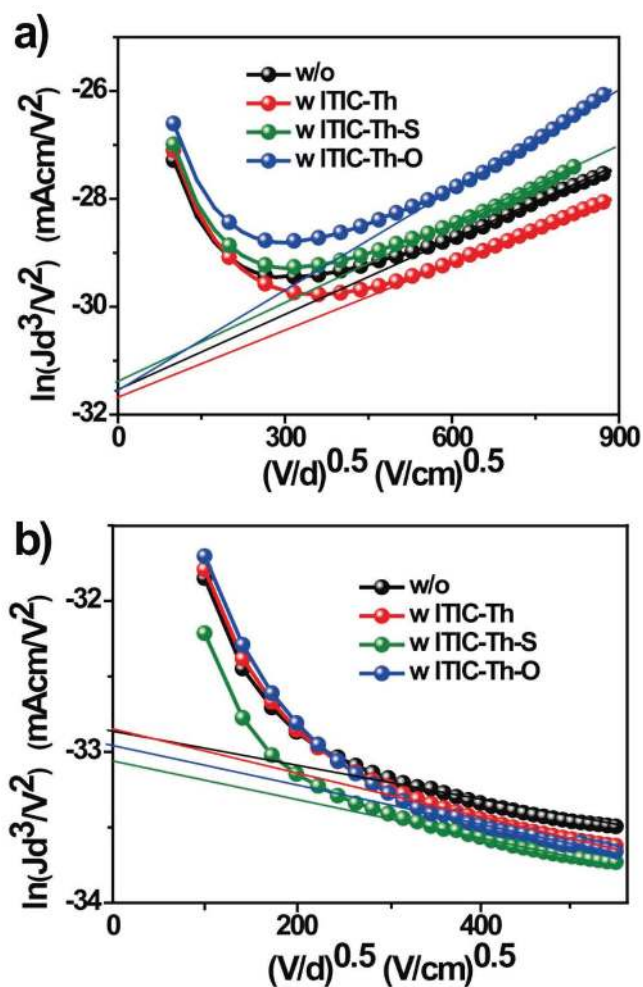
**ADVANCED
SCIENCE NEWS**
www.advancedsciencenews.com

**ADVANCED
MATERIALS**
www.advmat.de

Figure 7. a) Hole-only and b) electron-only devices based on FTAZ/IDIC blend films without or with different third components.

Table 2. Hole and electron mobilities of FTAZ/IDIC blend films without or with different third components (average by five devices).

Active layer	μ_h [cm^2 V^{-1} s^{-1}]	μ_e [cm^2 V^{-1} s^{-1}]
FTAZ/IDIC	$1.2 \pm 0.4 \times 10^{-4}$	$3.4 \pm 1.5 \times 10^{-5}$
FTAZ/ITIC-Th/IDIC	$1.0 \pm 0.3 \times 10^{-4}$	$3.4 \pm 1.4 \times 10^{-5}$
FTAZ/ITIC-Th-S/IDIC	$1.4 \pm 0.4 \times 10^{-4}$	$2.6 \pm 1.2 \times 10^{-5}$
FTAZ/ITIC-Th-O/IDIC	$1.2 \pm 0.4 \times 10^{-4}$	$2.9 \pm 1.4 \times 10^{-5}$

wide-angle X-ray scattering (GIWAXS) and transmission electron microscopy (TEM) measurements were carried out. GIWAXS provides molecular-level structural information such as lattice constant and orientation of molecular packing, while TEM provides larger length-scale phase separation information up to hundreds of nanometers. **Figure 6** shows 2D GIWAXS patterns of FTAZ/IDIC films without or with different third components (ITIC-Th, ITIC-Th-S, and ITIC-Th-O). The out-of-plane and in-plane line cuts are shown in Figure S4 (Supporting information). The molecular packing behavior in binary blend film and all ternary blend films was similar in terms of molecular crystallite orientation and aggregation. At the same time, these binary blend and ternary blend films exhibited similar scale of phase separation, which is apparent in TEM images (Figure S5, Supporting information). Thus, the film morphology of FTAZ/IDIC active layer without or with these ITIC-Th based third components was shown to be similar at both molecular-level and hundreds of nanometers scale. This suggests that the employment of third component with good compatibility (structurally similar to acceptor) can maintain the optimized film morphology of active layer.

The space charge limited current (SCLC)[55] method was employed to measure the hole and electron mobility of binary and ternary blend films. Hole-only and electron-only diodes were fabricated using the architectures of indium tin oxide (ITO)/poly(3,4-ethylenedioxythiophene): poly(styrene sulfonate) (PEDOT: PSS)/active layer/gold (Au) for holes and aluminum (Al)/active layer/Al for electrons. The dark J–V curves of the devices are plotted as $\ln[Jd^3/(V_{appl} - V_{bi})^2]$ versus $[(V_{appl} - V_{bi})/d]^{0.5}$ in **Figure 7**. The average hole and electron mobilities are calculated and listed in **Table 2**. Thanks to preserved optimized film morphology of active layer, the average hole and electron mobilities of the binary blend and all ternary blend films were shown to be similar (1.0–1.4 × 10^{-4} cm^2 V^{-1} s^{-1} for hole; 2.6–3.4 × 10^{-5} cm^2 V^{-1} s^{-1} for electron).

In summary, two new nonfullerene acceptors ITIC-Th-S and ITIC-Th-O were designed, synthesized and employed as a third component in the blend of donor FTAZ/acceptor IDIC. Through chemical modification, the HOMO energy level of the third component was up-shifted from −5.61 eV (ITIC-Th) to −5.41 eV (ITIC-Th-S)/ −5.36 eV (ITIC-Th-O), which is similar to that of the donor FTAZ (−5.35 eV); and the LUMO energy level of the third component was down-shifted from −3.81 eV (ITIC-Th) to −3.86 eV (ITIC-Th-S)/ −3.91 eV (ITIC-Th-O), which is similar to that of the acceptor IDIC (−3.91 eV). The up-shifted HOMO energy level and down-shifted LUMO energy level of the third component was able to narrow the bandgaps and broaden the absorption of active layer into the NIR region. Meanwhile,

(6:1, same as the value in the best FTAZ/ITIC-Th-O/IDIC ternary device) is much larger than that of the pure IDIC or pure ITIC-Th-O based cells, which should be attributed to the effective charge transfer between IDIC and ITIC-Th-O. The steady state photoluminescence (PL) was carried out to investigate the charge transfer in active layer. The PL intensities of FTAZ/IDIC films without or with different third components (ITIC-Th, ITIC-Th-S, and ITIC-Th-O) are shown in **Figure 5** (excite at 660 nm). Considering the absorption edge of FTAZ is at 630 nm, the PL peak at 760 nm of FTAZ/IDIC blend film is assigned to IDIC. Compared with FTAZ/IDIC binary blend film, the PL intensity of ternary blend films decreased by 70% (the PL intensities of different films were compared at their PL peaks). The stronger PL quenching of IDIC can mainly be caused by extra photoinduced hole transfer from IDIC to donor FTAZ or to third components, which suggests a more efficient charge transfer in the active layer. The more efficient charge transfer in ternary blend active layer is attributed to the formation of the optimized energy level alignment, which consequently enhances the J_{SC} and PCE of OPV.

In order to compare the film morphology of FTAZ/IDIC active layer without or with third component, grazing-incidence

**ADVANCED
SCIENCE NEWS**
www.advancedsciencenews.com

**ADVANCED
MATERIALS**
www.advmat.de

the optimized energy level alignment induces a more efficient charge transfer. In addition, due to similar chemical structure of these third components to the acceptor, these materials exhibited a good compatibility which can maintain the optimized film morphology of active layer at both molecular-level and hundreds of nanometers-scale. As a result, the broadened absorption and enhanced charge transfer can contribute to J_{SC} which are the reasons for the higher performance of FTAZ/ITIC-Th-O/IDIC ternary system compared with that of FTAZ/IDIC binary system. The best PCE of FTAZ/ITIC-Th-O/IDIC ternary blend OPV was measured to be 11.6%, which is higher than that of the controlled FTAZ/IDIC binary blend OPV (10.4%).

Supporting Information

Supporting Information is available from the Wiley Online Library or from the author.

Acknowledgements

Conflict of Interest

The authors declare no conflict of interest.

Keywords

[1] C. J. Brabec, M. Heeney, I. McCulloch, J. Nelson, *Chem. Soc. Rev.* **2011**, *40*, 1185.

[2] P. Cheng, G. Li, X. Zhan, Y. Yang, *Nat. Photonics* **2018**, *12*, 131.

[3] G. Li, R. Zhu, Y. Yang, *Nat. Photonics* **2012**, *6*, 153.

[4] M. Graetzel, R. A. J. Janssen, D. B. Mitzi, E. H. Sargent, *Nature* **2012**, *488*, 304.

[5] Y. F. Li, *Acc. Chem. Res.* **2012**, *45*, 723.

[6] J. Peet, A. J. Heeger, G. C. Bazan, *Acc. Chem. Res.* **2009**, *42*, 1700.

[7] J. Zhao, Y. Li, G. Yang, K. Jiang, H. Lin, H. Ade, W. Ma, H. Yan, *Nat. Energy* **2016**, *1*, 15027.

[8] G. A. Chamberlain, *Solar Cells* **1983**, *8*, 47.

[9] S. R. Forrest, *Nature* **2004**, *428*, 911.

[10] J. J. M. Halls, C. A. Walsh, N. C. Greenham, E. A. Marseglia, R. H. Friend, S. C. Moratti, A. B. Holmes, *Nature* **1995**, *376*, 498.

[11] G. Yu, J. Gao, J. C. Hummelen, F. Wudl, A. J. Heeger, *Science* **1995**, *270*, 1789.

[12] T. Ameri, P. Khoram, J. Min, C. J. Brabec, *Adv. Mater.* **2013**, *25*, 4245.

[13] L. Lu, M. A. Kelly, W. You, L. Yu, *Nat. Photonics* **2015**, *9*, 491.

[14] B. M. Savoie, S. Dunaisky, T. J. Marks, M. A. Ratner, *Adv. Energy Mater.* **2015**, *5*, 1400891.

[15] W. Huang, P. Cheng, Y. Yang, G. Li, Y. Yang, *Adv. Mater.* **2018**, *30*, 1705706.

[16] H. Xu, H. Ohkita, Y. Tamai, H. Benten, S. Ito, *Adv. Mater.* **2015**, *27*, 5868.

[17] J.-S. Huang, T. Goh, X. Li, M. Y. Sfeir, E. A. Bielinski, S. Tomasulo, M. L. Lee, N. Hazari, A. D. Taylor, *Nat. Photonics* **2013**, *7*, 479.

[18] P. P. Khlyabich, B. Burkhart, B. C. Thompson, *J. Am. Chem. Soc.* **2012**, *134*, 9074.

[19] L. Yang, H. Zhou, S. C. Price, W. You, *J. Am. Chem. Soc.* **2012**, *134*, 5432.

[20] L. Lu, T. Xu, W. Chen, E. S. Landry, L. Yu, *Nat. Photonics* **2014**, *8*, 716.

[21] Y. Yang, W. Chen, L. Dou, W.-H. Chang, H.-S. Duan, B. Bob, G. Li, Y. Yang, *Nat. Photonics* **2015**, *9*, 190.

[22] N. Gasparini, X. Jiao, T. Heumueller, D. Baran, G. J. Matt, S. Fladischer, E. Spiecker, H. Ade, C. J. Brabec, T. Ameri, *Nat. Energy* **2016**, *1*, 16118.

[23] R. Yu, S. Zhang, H. Yao, B. Guo, S. Li, H. Zhang, M. Zhang, J. Hou, *Adv. Mater.* **2017**, *29*, 1700437.

[24] G. Chen, H. Sasabe, X.-F. Wang, Z. Hong, J. Kido, *Synth. Met.* **2014**, *192*, 10.

[25] Z. Li, X. Xu, W. Zhang, X. Meng, Z. Genene, W. Ma, W. Mammo, A. Yartsev, M. R. Andersson, R. A. J. Janssen, E. Wang, *Energy Environ. Sci.* **2017**, *10*, 2212.

[26] X. Xu, Z. Bi, W. Ma, Z. Wang, W. C. H. Choy, W. Wu, G. Zhang, Y. Li, Q. Peng, *Adv. Mater.* **2017**, *29*, 1704271.

[27] P. P. Khlyabich, B. Burkhart, B. C. Thompson, *J. Am. Chem. Soc.* **2011**, *133*, 14534.

[28] T. M. Grant, T. Gorisse, O. J. Dautel, G. Wantz, B. H. Lessard, *J. Mater. Chem. A* **2017**, *5*, 1581.

[29] P. Cheng, M. Zhang, T.-K. Lau, Y. Wu, B. Jia, J. Wang, C. Yan, M. Qin, X. Lu, X. Zhan, *Adv. Mater.* **2017**, *29*, 1605216.

[30] J. M. Lee, B.-H. Kwon, H. I. Park, H. Kim, M. G. Kim, J. S. Park, E. S. Kim, S. Yoo, D. Y. Jeon, S. O. Kim, *Adv. Mater.* **2013**, *25*, 2011.

[31] M. Han, H. Kim, H. Seo, B. Ma, J.-W. Park, *Adv. Mater.* **2012**, *24*, 6311.

[32] S. Liu, P. You, J. Li, J. Li, C.-S. Lee, B. S. Ong, C. Surya, F. Yan, *Energy Environ. Sci.* **2015**, *8*, 1463.

[33] Y. Huang, W. Wen, S. Mukherjee, H. Ade, E. J. Kramer, G. C. Bazan, *Adv. Mater.* **2014**, *26*, 4168.

[34] Q. Wei, T. Nishizawa, K. Tajima, K. Hashimoto, *Adv. Mater.* **2008**, *20*, 2211.

[35] J. W. Jung, J. W. Jo, W. H. Jo, *Adv. Mater.* **2011**, *23*, 1782.

[36] Z. Xiao, Q. Dong, P. Sharma, Y. Yuan, B. Mao, W. Tian, A. Gruverman, J. Huang, *Adv. Energy Mater.* **2013**, *3*, 1581.

[37] P. Cheng, R. Wang, J. Zhu, W. Huang, S.-Y. Chang, L. Meng, P. Sun, H.-W. Cheng, M. Qin, C. Zhu, X. Zhan, Y. Yang, *Adv. Mater.* **2018**, *30*, 1705243.

[38] P. Cheng, C. Yan, Y. Wu, J. Wang, M. Qin, Q. An, J. Cao, L. Huo, F. Zhang, L. Ding, Y. Sun, W. Ma, X. Zhan, *Adv. Mater.* **2016**, *28*, 8021.

[39] P. Cheng, C. Yan, T.-K. Lau, J. Mai, X. Lu, X. Zhan, *Adv. Mater.* **2016**, *28*, 5822.

[40] D. Baran, R. S. Ashraf, D. A. Hanifi, M. Abdelsamie, N. Gasparini, J. A. Rohr, S. Holliday, A. Wadsworth, S. Lockett, M. Neophytou,

**ADVANCED
SCIENCE NEWS**

www.advancedsciencenews.com

**ADVANCED
MATERIALS**

www.advmat.de

C. J. M. Emmott, J. Nelson, C. J. Brabec, A. Amassian, A. Salleo, T. Kirchartz, J. R. Durrant, I. McCulloch, *Nat. Mater.* **2017**, *16*, 363.

[41] B. C. Schroeder, Z. Li, M. A. Brady, G. C. Faria, R. S. Ashraf, C. J. Takacs, J. S. Cowart, D. T. Duong, K. H. Chiu, C.-H. Tan, J. T. Cabral, A. Salleo, M. L. Chabinyc, J. R. Durrant, I. McCulloch, *Angew. Chem., Int. Ed.* **2014**, *53*, 12870.

[42] L. Derue, O. Dautel, A. Tournebize, M. Drees, H. Pan, S. Berthumeyrie, B. Pavageau, E. Cloutet, S. Chambon, L. Hirsch, A. Rivaton, P. Hudhomme, A. Facchetti, G. Wantz, *Adv. Mater.* **2014**, *26*, 5831.

[43] B. Fan, W. Zhong, X.-F. Jiang, Q. Yin, L. Ying, F. Huang, Y. Cao, *Adv. Energy Mater.* **2017**, *7*, 1602127.

[44] T. Liu, Y. Guo, Y. Yi, L. Huo, X. Xue, X. Sun, H. Fu, W. Xiong, D. Meng, Z. Wang, F. Liu, T. P. Russell, Y. Sun, *Adv. Mater.* **2016**, *28*, 10008.

[45] H. Lu, J. Zhang, J. Chen, Q. Liu, X. Gong, S. Feng, X. Xu, W. Ma, Z. Bo, *Adv. Mater.* **2016**, *28*, 9559.

[46] X. Xu, Z. Li, J. Wang, B. Lin, W. Ma, Y. Xia, M. R. Andersson, R. A. J. Janssen, E. Wang, *Nano Energy* **2018**, *45*, 368.

[47] C. Groves, *Energy Environ. Sci.* **2013**, *6*, 1546.

[48] F. Machui, S. Rathgeber, N. Li, T. Ameri, C. J. Brabec, *J. Mater. Chem.* **2012**, *22*, 15570.

[49] Y. Lin, F. Zhao, Q. He, L. Huo, Y. Wu, T. C. Parker, W. Ma, Y. Sun, C. Wang, D. Zhu, A. J. Heeger, S. R. Marder, X. Zhan, *J. Am. Chem. Soc.* **2016**, *138*, 4955.

[50] F. Zhao, S. Dai, Y. Wu, Q. Zhang, J. Wang, L. Jiang, Q. Ling, Z. Wei, W. Ma, W. You, C. Wang, X. Zhan, *Adv. Mater.* **2017**, *29*, 1700144.

[51] S. C. Price, A. C. Stuart, L. Yang, H. Zhou, W. You, *J. Am. Chem. Soc.* **2011**, *133*, 4625.

[52] Y. Lin, Q. He, F. Zhao, L. Huo, J. Mai, X. Lu, C.-J. Su, T. Li, J. Wang, J. Zhu, Y. Sun, C. Wang, X. Zhan, *J. Am. Chem. Soc.* **2016**, *138*, 2973.

[53] Y. Lin, F. Zhao, Y. Wu, K. Chen, Y. Xia, G. Li, S. K. K. Prasad, J. Zhu, L. Huo, H. Bin, Z.-G. Zhang, X. Guo, M. Zhang, Y. Sun, F. Gao, Z. Wei, W. Ma, C. Wang, J. Hodgkiss, Z. Bo, O. Inganäs, Y. Li, X. Zhan, *Adv. Mater.* **2017**, *29*, 1604155.

[54] Q. An, F. Zhang, J. Zhang, W. Tang, Z. Deng, B. Hu, *Energy Environ. Sci.* **2016**, *9*, 281.

[55] G. G. Malliaras, J. R. Salem, P. J. Brock, C. Scott, *Phys. Rev. B* **1998**, *58*, 13411.